Influence of Cone-beam Computed Tomographic Scan Mode for Detection of Horizontal Root Fracture

Felipe Ferreira da Costa, DDS, PhD, Lucas Rodrigues Pinheiro, DDS, Otavio Shoiti Umetsubo, DDS, MS, Oséas dos Santos Júnior, DDS, Bruno Felipe Gaia, DDS, PhD, and Marcelo Gusmão Paraiso Cavalcanti, DDS, MS, PhD

Abstract

Introduction: The purpose of the present study was (1) to test the accuracy of a small-volume cone-beam computed tomographic (CBCT) device in detecting horizontal root fractures (HRFs) in teeth with and without an intracanal metallic post (IMP) and (2) to investigate the use of 2 different acquisition protocols of a CBCT device for HRF diagnosis. **Methods:** Forty endodontically treated teeth with and without an IMP were examined using PreXion 3D CBCT scanner (Terarecon, San Mateo, CA) with a 5-cm high and 5-cm diameter cylinder at 0.10-mm voxel reconstruction. Two observers analyzed the samples to determine the presence and location of HRFs. **Results:** Sensitivity values ranged from 0.40–0.80. The most favorable results were found for the samples with no IMP observed using the protocol of a higher number of x-ray projections (0.70–0.80). Accuracy in the groups with an IMP ranged from 75%–90% in the 1024 x-ray projection protocol (HI-HI group) versus 70%–85% for the same samples examined in the 512 x-ray projection protocol (HI-STD group). Intraobserver agreement ranged from relevant to perfect concordance for both protocols (HI-HI = Kappa: 0.60–1.00 and HI-STD = Kappa: 0.55–0.89). Interobserver agreement ranged from moderate to perfect concordance for both protocols (HI-HI = Kappa: 0.79–0.89 and HI-STD = Kappa: 0.42–0.76). **Conclusions:** Even though there are statistically significant differences for the protocol with the higher number of x-ray projections, we found high accuracy, sensitivity, sensibility, and intra- and interobserver agreement in detecting HRFs for both Prexion 3D protocols. *(J Endod 2014;■:1–5)*

Key Words

Cone-beam computed tomography, diagnosis, horizontal root fracture

From the Department of Stomatology, College of Dentistry, University of São Paulo, São Paulo, Brazil.

Address requests for reprints to Prof Marcelo Cavalcanti, Av Lineu Prestes, 2227 Cidade Universitária, FOUSP, CEP 05508-900 São Paulo, SP, Brazil. E-mail address: mgpcaval@usp.br

0099-2399/$ - see front matter

http://dx.doi.org/10.1016/j.joen.2014.03.001

Radiographic examination is an important complementary examination for clinical diagnosis in endodontics (1). The need for better diagnostic imaging has driven radiographic techniques to achieve great developments, which are currently represented by 3-dimensional images.

Since its introduction in dentistry in 1999 by Arai et al (2), cone-beam computed tomographic (CBCT) imaging has proven to be of great importance and has attracted interest among dental professionals. Since then, dentistry has gained a 3-dimensional radiographic technique of high spatial resolution and low radiation dose compared with helicoidal computed tomographic imaging (3).

Root fractures represent a challenge to dental treatment. Clinical and radiographic examinations are of utmost importance for effective diagnosis. Two-dimensional images have limitations in representing 3-dimensional structures, which can hinder the diagnosis of horizontal root fractures (HRFs). CBCT imaging presents more accurate results than 2-dimensional examinations (4–6) because it allows clearer visualization (without superimposition of images) of the fracture lines.

Objects having high density, such as intracanal metallic posts (IMPs), guttapercha, and metallic restorations, produce artifacts generated by beam hardening when submitted to CBCT examination. These may interfere with the quality of the images to the extent of seriously compromising the endodontic diagnosis in some cases (4–8).

x-rays in more attenuated energy ranges are referred to as soft x-rays, whereas those in ranges that are more penetrating are referred to as hard x-rays. Thus, beam hardening is the process of selectively removing soft x-rays from the x-ray beam. As these x-ray are removed, the beam becomes progressively harder or more penetrating. Two types of artifacts can result from this effect: the so-called cupping artifacts and the appearance of dark bands or streaks between dense objects in the image.

Scan settings, including size of field of view (FOV), number of basis projections (acquisitions used to create the raw data), and scan mode (peak tube potential, current, and scan time in seconds), are among the most important factors in determining image quality and radiation dose levels for CBCT imaging (8, 9). The aims of the present study were (1) to test the accuracy of small-volume CBCT imaging in detecting HRFs in teeth with and without an IMP and (2) to investigate the use of 2 different acquisition protocols of a CBCT device for diagnosing HRFs. Our null hypothesis was that the use of a higher radiation dose protocol could influence the accuracy of HRF detection positively.

Materials and Methods

Preparation of Samples

With the approval of the Research Ethics Committee of the University of São Paulo, School of Dentistry, São Paulo, Brazil, 20 jaws and 40 single-rooted premolars were used. During the selection of the samples, teeth that had root resorption and fractures were excluded from the study.

The anatomic crowns of all the teeth were sectioned perpendicular to the long axis at the cementoenamel junction using water-cooled diamond burs propelled by an air turbine (300,000 rpm). The same operator, who was not involved in interpreting the images, performed endodontic treatment using #4 and #3 Gates Glidden drills, #40 and #30 Nitiflex files (Dentsply Maillefer, Ballaigues, Switzerland), obturation with sealer

TABLE 1. HI-HI Sensitivity and Specificity Coefficients and Accuracy Rates and Intraobserver Agreement on the Diagnosis of HRFs in Groups of Teeth without and with Metallic Posts

Observer 1							Observer 2						
First observation			Second observation				First observation			Second observation			
Se	Sp	A (%)	Se	Sp	A (%)	Agr	Se	Sp	A (%)	Se	Sp	A (%)	Agr
Samples without metallic post													
0.80	1.0	90	70	1.0	85	0.89	0.70	1.0	85	0.70	1.0	85	1.0
Samples with metallic post													
0.80	1.0	90	0.60	0.90	75	0.68	0.80	1.0	90	0.80	0.80	80	0.60

A, accuracy; Agr, agreement; C, circumferencial images; MPR, multiplanar reconstruction; P, parasagittal images; Se, sensitivity; Sp, specificity.

(Pulp Canal Sealer EWT; Sybron Endo, Orange, CA), and gutta-percha points (Dentsply Maillefer). All fillings were removed from the root canals up to two thirds of their length. Afterward, a post was modeled within each root canal. Root fracture was then caused in the teeth ($n = 20$) by applying a mechanical force on their horizontal plane using a hammer. The teeth were then placed on a soft foundation as previously described by Costa et al (10), Hassan et al (11), and Wenzel and Kirkevang (12). Teeth that were broken into 2 fragments were then assembled and glued without displacement. Teeth ($n = 6$) that broke into more than 2 fragments were replaced according to the inclusion criteria. The entire sample was kept hydrated during the process, except during fracture induction.

Image Acquisition

A water-filled plastic container was used as the head phantom to be imaged in order to simulate the attenuation of x-rays promoted by the soft tissues as previously used by Costa et al (10, 13), Moreira et al (14), Katsumata et al (15, 16), and Noujeim et al (17). A CBCT scan (PreXion 3D CBCT; Terarecon, San Mateo, CA) was performed for each tooth individually, and the teeth were then placed in the empty mandibular sockets of 20 human dry mandibles to obtain 2 different acquisition protocols (1024 and 512 x-ray projections). Thus, this CBCT device generated 1024 basis projections to create raw data for the first protocol and then 512 basis projections for the second protocol.

Both scanning protocols had the same machine parameters of 90 kV(p) and 4 mA and the same small FOV. The limits of the imaging area consisted of a 5-cm high and 5-cm diameter cylinder with 0.10-mm voxel reconstruction. Afterward, the cobalt-chromium metallic posts were inserted into the root canals, and the teeth were scanned again following the same protocols.

Accordingly, 20 CBCT scans of roots with a metallic post and an equal number of images without a metallic post (each group containing 20 teeth with a fracture and 20 with no fracture) were obtained for each protocol. Thus, the CBCT readers examined 80 samples.

The scans were coded and divided into 4 groups of teeth for each protocol: with neither IMP nor HRF (G1), without IMP but with HRF (G2), with IMP but without HRF (G3), and with both IMP and HRF (G4). Therefore, each of the 2 double-blinded observers, who were oral and maxillofacial radiologists trained and calibrated on tomographic features of HRF, analyzed 80 CBCT scans in each observation. After image acquisition, the data were imported into a specially designed open-source DICOM viewer for the MacOS OsiriX 5.6 32-bit version (Pixmeo, Geneva, Switzerland; http://www.osirix-viewer.com/).

The observers had access to all the features available in this software and could observe multiplanar reconstructed images (axial, coronal, and sagittal) as well as parasagittal and circumferential images. The observer had to identify the location of the fracture on the root surface (cervical, middle, or apical). Incorrect locations were considered as misdiagnoses. After 2 weeks, a second observation was made to evaluate intraobserver agreement. The sequence of observations was randomized by a software application (Randomness 1.5.2; Andrew Merenbach, Los Angeles, CA) (Fig. 1).

Results

Table 1 shows the results for sensitivity, specificity, accuracy, and intraobserver agreement in the samples observed with the protocol of 1024 x-ray projections (HI-HI). Sensitivity values (in this case, representing the most appropriate examination to identify the HRF) of the samples without a metallic post ranged from 0.70–0.80. On the other hand, sensitivity values of samples with a metallic post ranged from 0.6–0.80. The results for accuracy, represented as the total number of true positives and true negatives, that were found for the samples with no metallic post ranged between 85% and 90% versus 75% and 90% for the samples with a metallic post. The intraobserver agreement for the samples with no metallic post was found to be 0.89 and 1.0 (very strong agreement) versus 0.6 and 0.68 (relevant concordance) for the metallic post samples.

TABLE 2. HI-STD Sensitivity and Specificity Coefficients and Accuracy Rates and Intraobserver Agreement on Diagnosis of HRF in Groups of Teeth without and with Metallic Posts

Observer 1							Observer 2						
First observation			Second observation				First observation			Second observation			
Se	Sp	A (%)	Se	Sp	A (%)	Agr	Se	Sp	A (%)	Se	Sp	A (%)	Agr
Samples without metallic post													
0.70	1.0	85	0.60	1.0	80	0.89	0.67	1.0	0.79	0.80	0.90	80	0.55
Samples with metallic post													
0.60	1.0	80	0.40	1.0	70	0.73	0.60	1.0	80	0.80	0.90	85	0.69

A, accuracy; Agr, agreement; C, circumferencial images; MPR, multiplanar reconstruction; P, parasagittal images; Se, sensitivity; Sp, specificity.

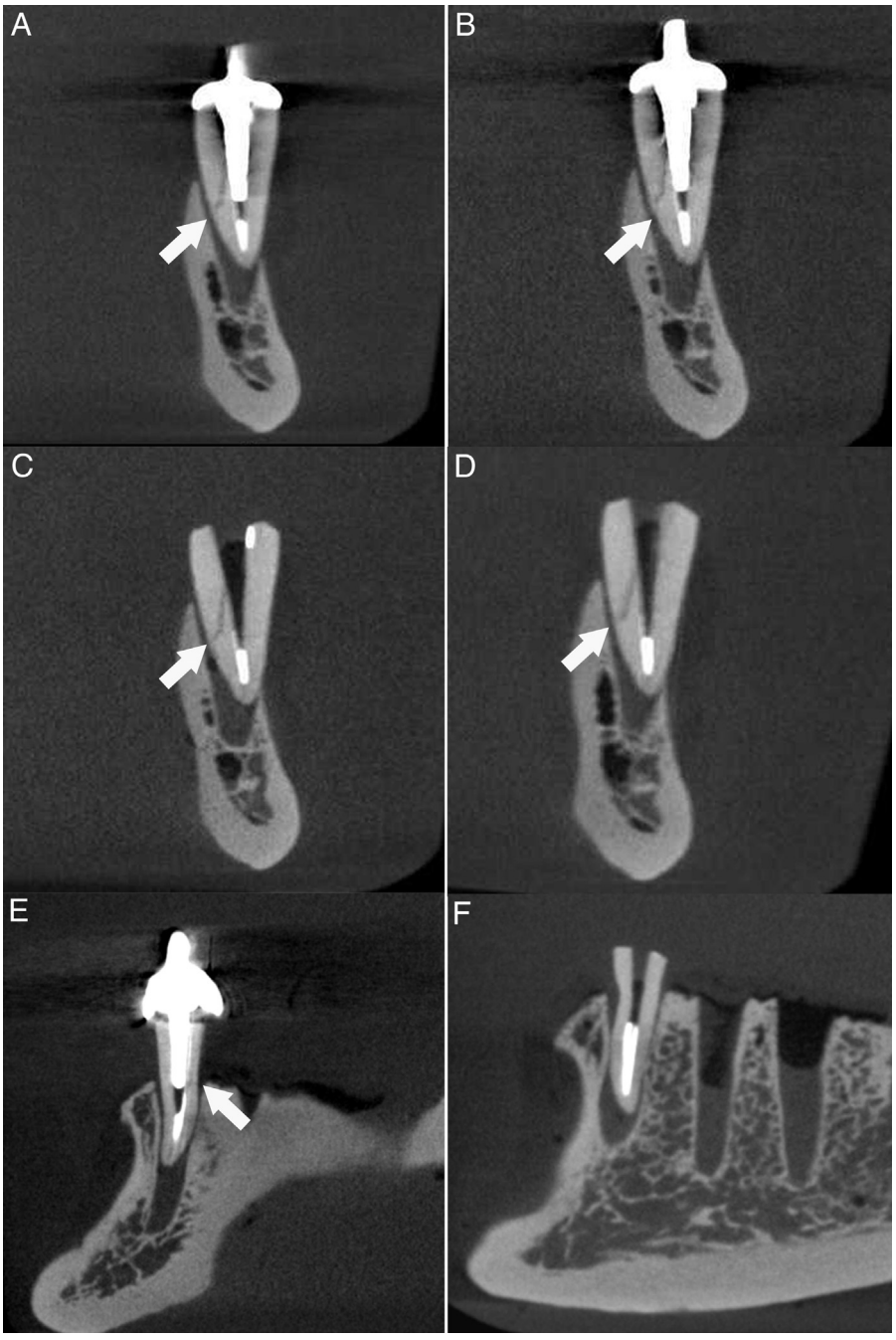

Figure 1. Circumferential CBCT images. (*A* and *B*) A sample with a horizontal root fracture and a metallic post (*arrow*). (*C* and *D*) A sample with a horizontal root fracture without a metallic post (*arrow*). (*E*) A sample without a horizontal root fracture with a radiolucent image caused by a metallic artifact (*arrow*). (*F*) A sample without a horizontal root fracture and a metallic post.

Table 2 shows the results for sensitivity, specificity, accuracy, and intraobserver agreement for the samples observed with the protocol of 512 x-ray projections (HI-STD). The sensitivity of the sample with no metallic post ranged from 0.67–0.70 versus 0.40–0.80 for samples with a metallic post. The accuracy for the samples with no metallic post ranged between 79% and 85% versus 70% and 85% for the samples with a metallic post. In the HI-STD protocol, the intraobserver agreement for the samples with no metallic post was 0.55 and 0.89 (moderate agreement and very strong) versus 0.69 and 0.73 (relevant concordance) for the metallic post samples.

In relation to interobserver concordance in the HI-HI protocol, the results obtained were 0.89 in the analysis of samples with no IMP versus 0.79 for samples with an IMP. In the HI-STD protocol, the results were 0.41 and 0.76, respectively.

Discussion

There are different acquisition and postacquisition protocols for 3-dimensional examination in the same CBCT scanner. Different sizes of FOV and acquisition times may influence the quality of a computed tomographic scan and the radiation dose delivered to the patient. An

understanding of CBCT technology, including its properties and limitations, is essential in preventing misleading findings (18).

Small-volume CBCT scans are known to generate images with higher resolution compared with large-volume CBCT scans (8); this is an important attribute for detecting root fracture. Bechara et al (19) claims that a large-volume CBCT scan did not increase the diagnostic accuracy of root fracture in endodontically treated teeth compared with a digital 2-dimensional intraoral radiography system. Because image quality is proportional to dose, the selection of image quality becomes a dose-related decision (20).

In this study, we used same small-volume CBCT equipment to perform all scans; nevertheless, this equipment allows changes in the number of x-ray projections. An increased number of projections exposes the patient to greater amounts of radiation. Thus, the effort to get better quality images represents a major biological cost.

According to Ludlow and Ivanovic (20), the Prexion 3D high-resolution protocol (HI-HI) represents a 388-μSv effective dose and the standard resolution protocol a 189-μSv effective dose. Pauwels et al (21) performed effective dose measurements with 14 different CBCT devices. The measurements resulted in values between 19 and 368 μSv depending on the selected volume size and/or position. Rottke et al (22) calculated the effective dose for 10 different CBCT devices. This calculation resulted in values between 17.2 and 396 μSv. The mean value for the protocols with the lowest exposure parameters was 31.6 μSv versus 209 μSv for the protocols with the highest exposure parameters.

Incorrect equipment selection could result in the equipment delivering unacceptably high patient doses for certain imaging procedures. This is particularly important when the exposure of children is involved, as is commonly the case in dental practice (23).

The occurrence of noise in tomographic images increases with the reduction in the number of x-ray beam photons. Accordingly, scans with low-dose radiation can generate tomographic images with a noise level that is inappropriate for observing HRF insofar as the noise may mimic fractures. The results obtained in this study corroborate this assertion (8). The sample specificity results, especially samples with no IMP, were more favorable for the HI-HI rather than the HI-STD protocol.

Our research using another small-volume CBCT device with the same methodology (10) found levels of accuracy ranging from 55%–70% for the samples with an IMP. In the present study, it ranged from 75%–90% (HI-HI protocol) to 70%–85% (HI-STD protocol). We found higher accuracy, sensitivity, and specificity values for both protocols used in this study compared with those of the previous study.

We believe that the combination of the reduced focal point (0.15 mm), small voxel (0.10 mm), and longer image acquisition time (19 or 37 seconds) of this small-volume CBCT device generated images with a higher resolution and, therefore, reduced the diagnostic interference caused by metallic artifacts. In this same small-volume CBCT scan, we found statistically significant differences in the samples with or without an IMP when using different protocols (HI-HI or HI-STD).

The sensitivity found in the observations of the samples with or without an IMP in the HI-HI protocol was higher than that found in the HI-STD protocol. This could mean that the observer would have a greater chance of identifying HRFs in the protocol with a higher acquisition time without an IMP.

The largest number of photons in the x-ray beam found in the HI-HI protocol examination compared with the HI-STD protocol can also explain the higher intraobserver agreement for the samples with and without a metallic post in the HI-HI protocol compared with the HI-STD protocol.

According to our studies (10, 13) and other studies (24, 25), we found more efficient results to warrant using the small-volume CBCT scan as a better alternative to using large-volume CBCT imaging in diagnosing HRFs. All exposures of ionizing radiation should follow the "as low as reasonably achievable" principle. For this reason, the selection criteria and the parameters for each CBCT scan protocol should be strict and should follow the respective clinical indication.

Conclusions

The CBCT device used in this study showed high accuracy, sensitivity, and specificity in both protocols used, even in samples with an IMP. The HI-HI protocol samples showed slightly higher sensitivity, specificity, and accuracy values compared with those of the HI-STD protocol samples. Another observation was that there was a smaller variance in the intra- and interobserver protocol when the samples were analyzed with the HI-HI protocol. For this reason, the null hypothesis was accepted.

Acknowledgments

Supported by the (CNPq National Council for Research, Dr. Marcelo Cavalcanti Research Productivity Scholarship), Brasilia, Brazil (grant no. 303847/2009-3 [to M.G.P.C.]), Universal Research Project (grant no. 472895/2009-5 [to M.G.P.C.]), CAPES (PhD scholarships to F.F.C., B.F.G., and O.S.U, and master's scholarship to O.S.J.), and FAPESP (PhD scholarship to L.R.P.).

The authors deny any conflicts of interest related to this study.

References

1. May JJ, Cohenca N, Peter AO. Contemporary management of horizontal root fractures to the permanent dentition: diagnosis—radiologic assessment to include cone-beam computed tomography. J Endod 2013;39:S20–5.
2. Arai Y, Tammisalo E, Iwai K, et al. Development of a compact computed tomographic apparatus for dental use. Dentomaxillofac Radiol 1999;28:245–8.
3. Metska ME, Aartman IH, Wesselink PR, Özok AR. Detection of vertical root fractures *in vivo* in endodontically treated teeth by cone-beam computed tomography scans. J Endod 2012;38:1344–7.
4. Barrett JF, Keat N. Artifacts in CT: recognition and avoidance. Radiographics 2004; 24:1679–91.
5. Perrella A, Lopes PM, Rocha RG, et al. Influence of dental metallic artifact from multislice CT in the assessment of simulated mandibular lesions. J Appl Oral Sci 2010; 18:149–54.
6. Junqueira RB, Verner FS, Campos CN, et al. Detection of vertical root fractures in the presence of intracanal metallic post: a comparison between periapical radiography and cone-beam computed tomography. J Endod 2013;39:1620–4.
7. Shemesh H, van Soest G, Wu MK, Wesselink PR. Diagnosis of vertical root fractures with optical coherence tomography. J Endod 2008;34:739–42.
8. Lee RD. Common image artifacts in cone beam CT. AADMRT Newsletter 2008:1-7.
9. Hassan B, Metska ME, Ozok AR, et al. Detection of vertical root fractures in endodontically treated teeth by a cone beam computed tomography scan. J Endod 2009;35:719–22.
10. Costa FF, Gaia BF, Umetsubo OS, Cavalcanti MG. Detection of horizontal root fracture with small-volume cone-beam computed tomography in the presence and absence of intracanal metallic post. J Endod 2011;37:1456–9.
11. Hassan BA, Payam J, Juyanda B, van der Stelt P, Wesselink PR. Influence of scan setting selections on root canal visibility with cone beam CT. Dentomaxillofac Radiol 2012;41:645–8.
12. Wenzel A, Kirkevang LL. High resolution charge-coupled device sensor vs. medium resolution photostimulable phosphor plate digital receptors for detection of root fractures *in vitro*. Dent Traumatol 2005;21:32–6.
13. Costa FF, Gaia BF, Umetsubo OS, et al. Use of large-volume cone-beam computed tomography in identification and localization of horizontal root fracture in the presence and absence of intracanal metallic post. J Endod 2012;38:856–9.
14. Moreira CR, Sales MA, Lopes PM, Cavalcanti MG. Assessment of linear and angular measurements on three-dimensional cone-beam computed tomographic images. Oral Surg Oral Med Oral Pathol Oral Radiol Endod 2009;108:430–6.
15. Katsumata A, Hirukawa A, Okumura S, et al. Relationship between density variability and imaging volume size in cone-beam computerized tomographic scanning of the maxillofacial region: an *in vitro* study. Oral Surg Oral Med Oral Pathol Oral Radiol Endod 2009;107:420–5.
16. Katsumata A, Hirukawa A, Okumura S, et al. Effects of image artifacts on gray-value density in limited-volume cone-beam computerized tomography. Oral Surg Oral Med Oral Pathol Oral Radiol Endod 2007;104:829–36.

17. Noujeim M, Prihoda T, Langlais R, Nummikoski P. Evaluation of high-resolution cone beam computed tomography in the detection of simulated interradicular bone lesions. Dentomaxillofac Radiol 2009;38:156–62.
18. Camilo CC, Brito-Junior M, Faria-E-Silva AL, et al. Artefacts in cone beam CT mimicking an Extrapalatal Canal of Root-Filled Maxillary Molar. Case Rep Dent 2013;2013:797286.
19. Bechara B, McMahan C, Noujeim M, et al. Comparison of cone beam CT scans with enhanced photostimulated phosphor plate images in the detection of root fracture of endodontically treated teeth. Dentomaxillofac Radiol 2013;42:20120404.
20. Ludlow JB, Ivanovic M. Comparative dosimetry of dental CBCT devices and 64-slice CT for oral and maxillofacial radiology. Oral Surg Oral Med Oral Pathol Oral Radiol Endod 2008;106:106–14.
21. Pauwels R, Beinsberger J, Collaert B, et al. Effective dose range for dental cone beam computed tomography scanners. Eur J Radiol 2012;81:267–71.
22. Rottke D, Patzelt S, Poxleitner P, Schulze D. Effective dose span of ten different cone beam CT devices. Dentomaxillofac Radiol 2013;42:20120417.
23. Horner K, Jacobs R, Schulze R. Dental CBCT equipment and performance issues. Radiat Prot Dosimetry 2013;153:212–8.
24. Kamburoglu K, Cebeci ARI, Grondahl HG. Effectiveness of limited cone-beam computed tomography in the detection of horizontal root fracture. Dent Traumatol 2009;25:256–61.
25. Kamburoglu K, Onder B, Murat S, et al. Radiographic detection of artificially created horizontal root fracture using different cone beam CT units with small fields of view. Dentomaxillofac Radiol 2013;42:20120261.